Fluorescence quenching and spectral diffusion in La$_{1-x}$P$_5$O$_{14}$:Nd$_x^{3+}$

M. M. Broer,* D. L. Huber, and W. M. Yen

Department of Physics, University of Wisconsin—Madison, Madison, Wisconsin 53706

W. K. Zwicker

Philips Laboratories, North American Philips Corporation, Briarcliff Manor, New York 10510

Donor-donor and donor-acceptor spectral dynamics are studied in the laser material La$_{1-x}$P$_5$O$_{14}$:Nd$_x^{3+}$ using time-resolved fluorescence line narrowing. Direct excitation in the $^4F_{3/2}(1)$ state in $x=0.2$, 0.75, and 1.0 samples shows exponential fluorescence decay and linear concentration quenching of the line-narrowed component between 4.5 and 20 K. No spectral diffusion across the inhomogeneously broadened line is observed in this temperature region. This unusual exponential decay and linear quenching in the absence of fast donor-donor transfer is explained with a generalized Inokuti-Hirayama model. An onset of spectral migration is observed in $x=0.2$ and 0.75 at 20 K, indicating the presence of phonon-assisted energy transfer. The temperature dependence of the phonon-assisted donor-donor transfer rate is measured for $x=0.2$ between 17 and 24 K. This temperature dependence identifies the one-site resonant process, with an activation energy corresponding to the $^4I_{9/2}(2)$-$^4I_{9/2}(1)$ splitting, as the probable donor-donor interaction mechanism. The low-temperature results and the spectral diffusion measurements are described consistently in the studied temperature range by phonon-assisted energy transfer models, in which the donor excitation is transferred between single ions in an incoherent manner.

I. INTRODUCTION

NdP$_5$O$_{14}$ was introduced[1] in 1972 as the first compound of a new class of crystalline Nd^{3+} laser materials which can be doped up to the stoichiometric limit without a significant loss in the fluorescence quantum efficiency (QE). The high Nd^{3+} concentration ($\approx 4 \times 10^{21}$ cm^{-3}) and the relatively unaffected QE result in a high optical gain per unit length. This has obvious advantages for miniature optical-device application. Lasing action in NdP$_5$O$_{14}$ and in the diluted system La$_{1-x}$P$_5$O$_{14}$:Nd$_x^{3+}$ (LNPP) has therefore extensively been investigated.[2,3] This technical application is directly related to the anomalous luminescence properties of LNPP. The fluorescence concentration quenching in LNPP is linearly dependent[4,5] on the fractional Nd^{3+} concentration x. In many other hosts[6] the quenching rate $q(x)$, with $q(x)=\tau_D^{-1}-\tau_0^{-1}$, varies as x^2 (τ_D^{-1} is the measured decay rate, after pulsed excitation, and τ_0^{-1} is the decay rate at very low Nd^{3+} concentration). The fluorescence from the upper laser level, the $^4F_{3/2}(1)$ state, decays exponentially with a temperature-independent decay rate between 2 and 300 K. This fluorescence behavior of LNPP is not well understood and an understanding of the underlying Nd^{3+}-Nd^{3+} interactions is necessary for the development of new, efficient phosphors and laser materials. From a more physical point of view, LNPP is an interesting case in the studies of optical excitation migration and trapping in disordered and stoichiometric systems.[7]

In this paper we investigate for the first time in a direct manner the spectral donor-donor and donor-acceptor dynamics in LNPP. Previous studies[4-6,8-10] employed nonresonant excitation of the near-ir $^4F_{3/2}(1)$ level. This excitation scheme suffers from accidental degeneracy[11] and hence results in broadband pumping of the $^4F_{3/2}(1)$ level. Several energy migration studies in other doped systems, both crystalline and amorphous, have shown[12] that direct excitation into the level of interest is required to extract the various donor-donor and donor-acceptor interaction mechanisms within the level. For this reason, we use the technique of time-resolved fluorescence line narrowing[12,13] (TRFLN) for selective excitation within the inhomogeneously broadened $^4F_{3/2}(1)$ state. The results are described along the lines of recent, similar energy-transfer studies.[7,12,14] The exponential decay and linear concentration quenching rate $q(x)$ were explained by fast donor-donor migration[5,9] using classical energy-transfer theories. These theories treat the indirectly excited $^4F_{3/2}(1)$ level as donors which are in resonance and ignore the small energy differences between them in the inhomogeneously broadened line. Energy transfer among the donors within this line generally shows a very strong temperature dependence,[12] so this explanation of fast migration is expected to break down at low temperatures. At low temperatures the donor-donor transfer is negligible in the case of phonon-assisted energy transfer, and the only remaining process in LNPP is trapping of the donor excitation by cross relaxation with an acceptor.[14] In disordered systems this process results in nonexponential fluorescence decay and a quadratic concentration quenching rate.[11,12,14] Various other explanations, including strong spatial migration in the absence of spectral diffusion[10,15] and excitonic effects,[16] have been suggested to explain the unusual exponential decay and linear quenching in LNPP. These models will be compared with the TRFLN measurements.

In Sec. II we describe the experimental techniques for

performing TRFLN resonantly in the $^4F_{3/2}(1)$ state. The results are presented in Sec. III. Low-temperature fluorescence decay and spectral diffusion measurements were reported in a previous publication[17] and will be reviewed briefly. The second part concerns the measurement of spectral donor-donor transfer at higher temperatures. The results will be analyzed with recently developed incoherent energy-transfer models and compared with other studies of the Nd^{3+}-Nd^{3+} interactions in LNPP.

II. EXPERIMENTAL DETAILS

In order to perform fluorescence line narrowing (FLN) resonantly in the $^4F_{3/4}(1)$ state, a narrowband and near-ir tunable source is required at ≈ 0.87 μm (a Nd^{3+} energy level diagram is shown in Fig. 1). This spectral region is not conveniently accessible to pulsed dye lasers with ir dyes. Therefore, the frequency of a yttrium aluminum garnet (YAG) pumped oscillator-preamplifier-amplifier dye laser was downshifted by stimulated Raman scattering in high-pressure H_2 gas. The linewidth of the dye laser is 5 GHz and the output pulse energy is approximately 25 mJ (5-ns pulse) at 10-Hz pulse repetition frequency. With DCM dye the first Stokes-shifted component was used for resonant excitation of the $^4F_{3/2}(1)$ level.

The single-crystal samples were cleaved along the (010) plane[18] and were mounted on the cold finger of a continuous-flow helium cryotip refrigerator. The temperature was measured with a Ge resistor and a feedback heater-controller system provided temperatures from 4.5 K upward. The incident, near-ir laser beam was suffi-

ciently atttenuated to prevent stimulated emission or ion pair effects[19] (Auger recombination). We applied TRFLN to $x=0.2$, 0.75, and 1.0 samples. The resonant $^4F_{3/2}(1)$ $\rightarrow ^4I_{9/2}(1)$ and nonresonant $^4F_{3/2}(1) \rightarrow ^4I_{11/2}(1)$ fluorescences (at 1.05 μm) were analyzed with a $1m$ Czerny-Turner spectrometer and detected with a Varian model-VPM159 InGaAsP photomultiplier tube (PMT).

The high Nd^{3+} concentration in the LNPP samples may cause overabsorption problems in the measurement of the $^4F_{3/2}(1)$ line shapes, so that excitation spectra were used by monitoring the nonresonant 1.05-μm fluorescence. The time development of the fluorescence was analyzed with standard gated integrator techniques using a Princeton Applied Research 162/164 boxcar. In the case of a weak signal (the resonant transition) a photon counting system was employed. Normalization of the fluorescence intensity against the laser-pulse amplitude was required because of the large shot-to-shot fluctuations in first Stokes output of the Raman shifter. A Digital Equipment Corporation LSI-11/2-microcomputer—based system[20] sampled for every shot the output of the boxcar (photon counter) and a photodiode which monitored the laser intensity. Signal normalization, averaging, display, and resetting of the boxcar and photon counter were also carried out by the computer. The spectral diffusion was measured from the decay of the initially excited ions (the FLN component) and the rise of the inhomogeneous background.[21]

The nonresonant fluorescence in all three concentrations showed residual broadening, which was too large compared to the inhomogeneous widths for a meaningful extraction of the FLN component. The resonant fluorescence does not suffer from this effect and was therefore used in the spectral diffusion measurements. Saturation of the PMT by scattered resonant laser light was prevented by a single chopper[22] which blocks the PMT during the laser pulse. In this chopper system the firing of the YAG laser is synchronized with the position of the chopper blade and it has a turn-on time of 2 μs.

III. RESULTS AND DISCUSSION

A. Spectral properties of LNPP

Before the spectral developments in the $^4F_{3/2}(1)$ state can be studied, the broadening mechanism of this level and the selective excitation of a subset of Nd^{3+} ions must be investigated. As mentioned previously, the high Nd^{3+} concentration in LNPP results in a large absorption coefficient:[17] 83 cm^{-1} at 4 K for $x=1.0$. Self-absorption and line reversal may distort the measured profile in an absorption measurement. This problem was avoided by measuring the excitation spectrum instead. A typical excitation profile of the $x=1.0$ sample at 6 K is shown in Fig. 2. The line is inhomogeneously broadened with no additional satellites outside the main line (except for a weak feature on the low-energy side). Similar single, inhomogeneous $^4F_{3/2}(1)$ line shapes were observed for the $x=0.2$ and 0.75 samples. The corresponding full widths at half maximum (FWHM) are shown in Table I. The excitation spectra show small shifts in the line peak position, which are dependent on the location of excitations in the
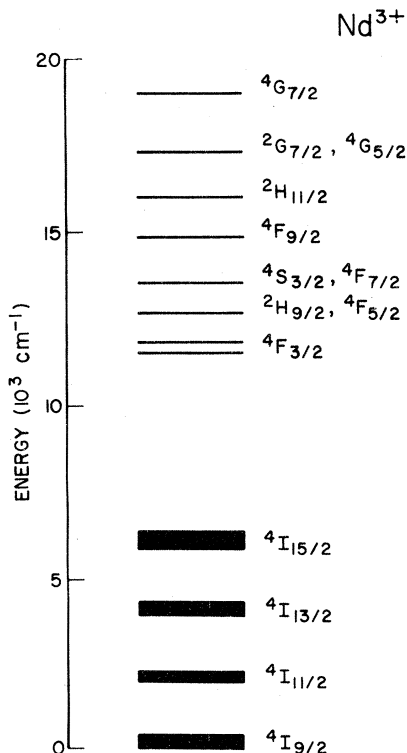

Nd^{3+}

Energy	Level
20	$^4G_{7/2}$
	$^2G_{7/2}$, $^4G_{5/2}$
	$^2H_{11/2}$
15	$^4F_{9/2}$
	$^4S_{3/2}$, $^4F_{7/2}$
	$^2H_{9/2}$, $^4F_{5/2}$
	$^4F_{3/2}$
10	
5	$^4I_{15/2}$
	$^4I_{13/2}$
	$^4I_{11/2}$
0	$^4I_{9/2}$

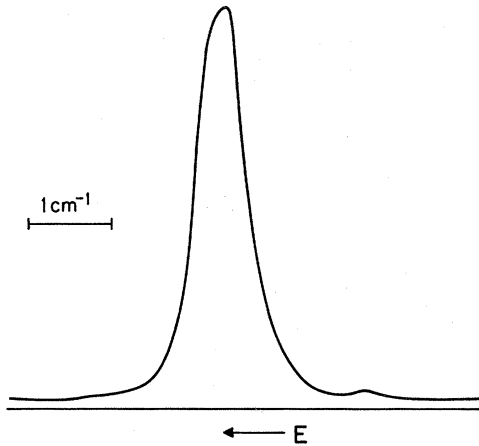ENERGY (10^3 cm^{-1})

FIG. 1. Energy levels of Nd^{3+} in LaP_5O_{14}.

FIG. 2. Excitation spectrum of the $^4I_{9/2}(1) \rightarrow {^4F_{3/2}}(1)$ transition in NdP_5O_{14} at 6 K.

crystal. This may indicate the presence of different domains inside the crystal. A weak, constant absorption outside the main line was observed in the $x=0.2$ and 1.0 samples (see Fig. 2). This continuous background did not appear in the rise of the inhomogeneous line in the spectral diffusion measurements. This background is not well understood, but may again reflect domains in the sample.

Both the resonant and nonresonant fluorescence show FLN in all three concentrations at low temperatures (5 K). The resonant fluorescence is spectrometer resolution limited, yet sufficiently resolved for isolation from the inhomogeneous background in the spectral dynamics studies. The narrowed, nonresonant components showed additional broadening due to accidental degeneracies,[21] which prevented their use in the spectral transfer measurements.[21] The decay of the FLN component in the three samples was exponential between 4.5 K and approximately 20 K, and the measured lifetimes at line center are shown in Table I. The consequence of this exponential decay and the absence of spectral developments in this temperature regime will be discussed below. Lifetime variations across the inhomogeneous line were observed in the three samples and an example for $x=0.2$ at 4.5 K is shown in Fig. 3. This variation indicates a corresponding spread in local Nd^{3+} concentrations,[23] which affects the lifetime through cross relaxation. This distribution of local Nd^{3+} concentrations is consistent with the earlier mentioned different domains in the crystal and complicates the analysis of the spectral diffusion measurements.

TABLE I. Inhomogeneous linewidths Δv_{inh} (FWHM) and line-center lifetime τ of the $^4F_{3/2}(1)$ state at $T=4.5$ K for different fractional Nd^{3+} concentrations x.

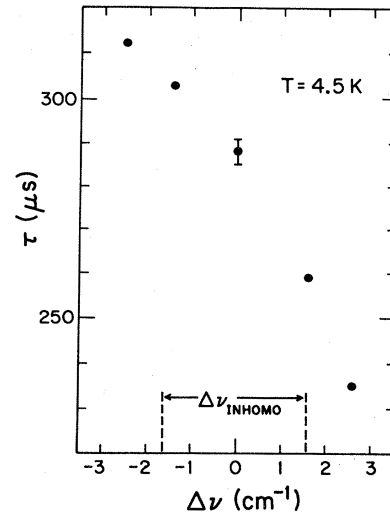| x	Δv_{inh} (cm^{-1})	τ (μs)
0.2	3.5	288
0.75	5.7	145
1.0	0.6	115

FIG. 3. Lifetime τ across the inhomogeneous line as a function of shift Δv in excitation from line center for $La_{0.8}Nd_{0.2}P_5O_{14}$. $T=4.5$ K.

B. Low-temperature TRFLN

The nonresonant excitation studies explained the exponential decay and linear quenching rate by assuming fast donor-donor migration. In this case τ_D^{-1} is given by[5,24]

$$\tau_D^{-1} = \tau_0^{-1} + x \sum_l{}' X_{0l} \tag{1}$$

with X_{0l} the trapping rate between a donor at site 0 and an acceptor at site l and $\sum_l{}'$ a sum over all lattice sites except the origin (site 0). The TRFLN measurements showed an exponential decay and a linear quenching rate $q(x)$ at 6 K for the $x=1.0$ sample and below 20 K for the $x=0.2$ and 0.75 samples. No spectral dynamics within the inhomogeneous line were observed over this temperature range for the three concentrations. This unusual combination of exponential decay and linear quenching and an absence of fast, spectral donor-donor transfer was discussed previously.[17] In the absence of donor-donor transfer the decay of the donor excitation in disordered systems is conveniently described by the quantity $R(t)$, which is the ratio of the integrated FLN line fluorescence intensity and the total integrated intensity at time t after the laser pulse:[17]

$$R(t) = \prod_l{}' [1 - x + x \exp(-X_{0l}t)] \tag{2}$$

with x and X_{0l} as before and $\prod_l{}'$ as a product over all lattice sites. This expression normally leads to a nonexponential fluorescence decay and a nonlinear quenching rate, and is a generalization[17] of the continuum Inokuti-Hirayama model. The absence of donor-donor transfer in LNPP at low temperatures is consistent with the exponential FLN decay because of the weak trapping in this compound.[17] In that case $R(t)$ in Eq. (2) can be approximated by a single exponential: $R(t) \approx \exp(-tx \sum_l{}' X_{0l})$. This implies a decay rate $\tau_D^{-1} = \tau_0^{-1} + x \sum_l{}' X_{0l}$, which is identical to the fast migration limit result in Eq. (1) and con-

sistent with the low-temperature TRFLN data.

The exponential decay in the absence of donor-donor transfer can be analyzed more quantitatively by explicitly calculating the expression for $R(t)$ in Eq. (2) in the following manner. The trapping rate X_{0l} can be written as

$$X_{0l} = X_{01}(R_{01}/R_{0l})^s \qquad (3)$$

with X_{01} the nearest-neighbor (NN) trapping rate and R_{01} the NN distance. In Eq. (3) an electric dipole-dipole interaction between donor and acceptor is assumed[5] ($s=6$). X_{01} can be derived from the room-temperature (RT) quenching rate data[5] of Lenth et al. if fast donor-donor transfer is assumed at this temperature. This is reasonable because of the observed onset of spectral diffusion at ≈ 20 K in the $x=0.2$ and 0.75 samples and the strong increase in the donor-donor transfer rate with increasing temperature.[12] In this limit Eqs. (1) and (3) are used to evaluate $X_{01}(T=300$ K) by carrying out the lattice sum in Eq. (1) over a sufficiently large number of sites. This sum involves the radial lattice site distribution in LaP_5O_{14}, which was calculated from the various crystallographic parameters of this host.[25,26] The temperature-independent decay rate τ_D^{-1} indicates a X_{01} which is also temperature independent, because of the large energy mismatch in the cross-relaxation process.[8] The value of X_{01} derived from the RT data in this manner can then be used as a first-order approximation for X_{01} in the low-temperature expression Eq. (2). By varying X_{01} an optimum fit of the data of Lenth et al. with the calculated decay rate from $R(t)$ [Eq. (2)] is obtained for $X_{01}=1.1x10^3$ s^{-1}.

The calculated values of $R(t)$ from Eq. (2) with this value of X_{01} are shown for several concentrations in Fig. 4. It is evident from these curves that for early times (compared to the radiative lifetime τ_0 which is ≈ 340 μs), the exact expression for $R(t)$ is characterized by a single
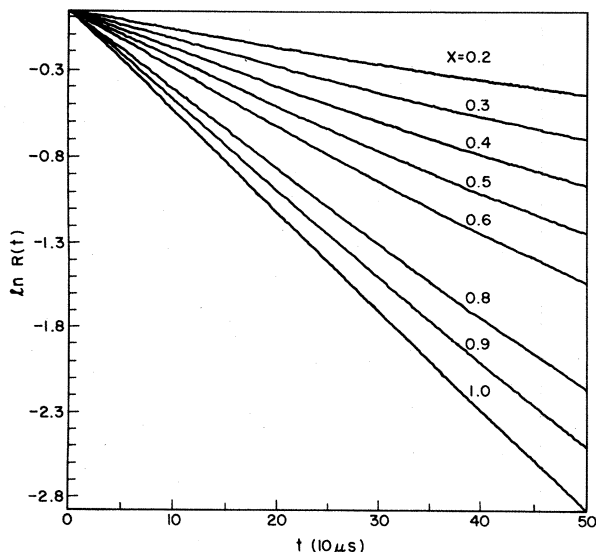
exponential decay, as was predicted from the earlier mentioned qualitative description of this early time regime. These calculated $R(t)$ values also yield[17] a linear concentration quenching rate for $0.01 < x < 1.0$ and do not show a break into a quadratic dependence, as was suggested recently.[15] Figure 5 shows the (calculated) time derivative of $R(t)$ for $x=0.2$ (with the same X_{01}), but now over a larger time interval. The deviation from a straight line at late times on this semilogarithmical plot illustrates the nonexponential decay for times longer than X_{0l}^{-1}, as mentioned before. However, this late-time regime is never reached because of the radiative decay: the trapping rate is sufficiently small in LNPP for the excited donor to have approximately equal probability to transfer its energy to a trap or to decay radiatively. Hence the observed exponential decay of the FLN component and linear quenching below 20 K are consistent with the absence of spectral diffusion and are described correctly by the expression for $R(t)$ in Eq. (3).

LNPP is the first compound, to our knowledge, which shows exponential fluorescence decay in the absence of fast donor-donor transfer because of the relative magnitude of the radiative decay rate and the (weak) trapping rate.

C. Spectral diffusion measurements

In the preceding section the NN trapping rate X_{01} was derived from the RT quenching rate data assuming fast donor-donor transfer at that temperature. This assumption follows from the observed spectral dynamics at approximately 20 K in both the $x=0.2$ and 0.75 samples. Spectral diffusion across the inhomogeneous line was observed at 20 K for $x=0.75$, as is shown in Fig. 6. The three time-resolved spectra show a rise in the inhomogeneous line which indicates transfer from the initially excited
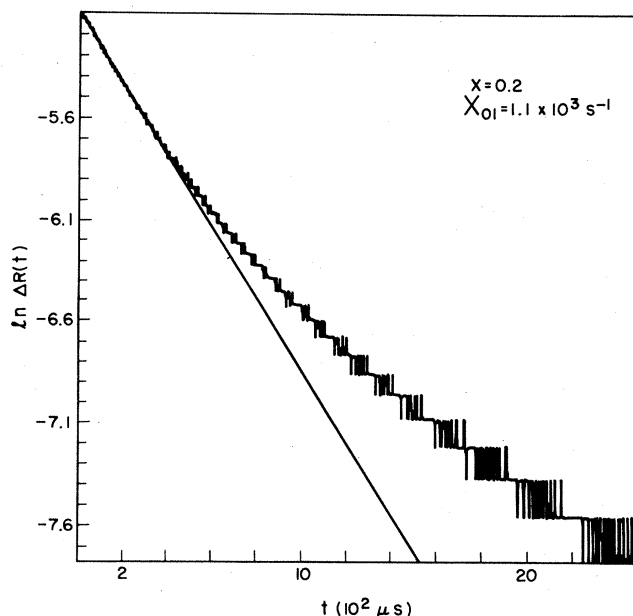
FIG. 4. Calculated $R(t)$ in the absence of donor-donor transfer for various concentrations x. $X_{01}=1.1\times10^3$ s^{-1}.

FIG. 5. Time derivative of $R(t)$ for $x=0.2$ and $X_{01}=1.1\times10^3$ s^{-1}.
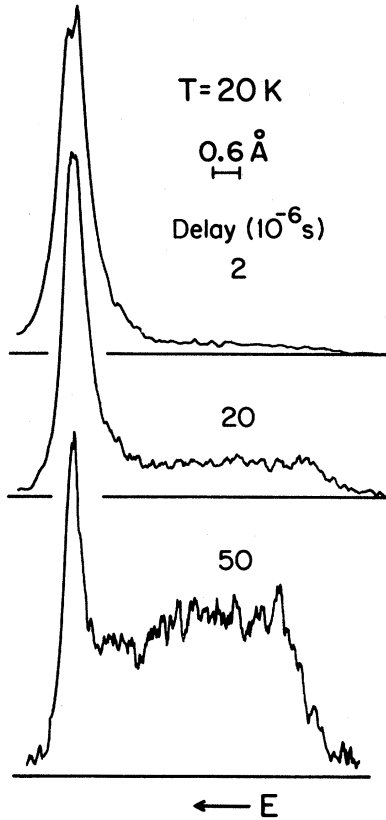
FIG. 6. TRFLN spectra in $La_{0.25}Nd_{0.75}P_5O_{14}$ at 20 K showing spectral diffusion across the inhomogeneous line.

FIG. 7. TRFLN spectra at 17 and 24 K for excitation at the center of the absorption line in $x=0.2$ sample ($\Delta\nu_{exc}=0$ cm^{-1}).

FLN component to the background. This measurement proved unambiguously that spectral diffusion occurs in LNPP and established, together with the absence of donor-donor spectral transfer below 20 K, the existence of phonon-assisted energy transfer in this compound.

The donor-donor transfer mechanism was investigated in detail by measuring the temperature dependence of the NN donor-donor transfer rate $W_{01}(T)$ in the $x=0.2$ sample. This transfer rate is extracted from the ratio $R(t)$ in the TRFLN spectra. Huber showed[24] that, in the presence of both donor-donor and donor-acceptor transfer via cross relaxation, $R(t)$ is given approximately by[27]

$$R(t)=\prod_{l}'\{1-x+x\exp[-(X_{0l}+W_{0l})t]\cosh(W_{0l}t)\}$$

(4)

with $\prod_{l}'$ and X_{0l} defined before and W_{0l} the transfer rate between a donor at site 0 and a donor at site l:

$$W_{0l}\equiv\frac{\beta}{(R_{0l})^s}=W_{01}\left[\frac{R_{01}}{R_{0l}}\right]^s.$$

(5)

The multipolarity of the donor-donor interaction is again s and R_{01} is as before.

The time-resolved $^4F_{3/2}(1)\rightarrow{}^4I_{9/2}(1)$ emission spectra of the $x=0.2$ sample, with excitation at the center of the excitation spectrum ($\Delta\nu_{exc}=0$ cm^{-1}), were recorded between 17 and 24 K and typical examples are shown in Fig. 7. These spectra clearly show the increase in the spectral diffusion with increasing temperature. Around 24 K the
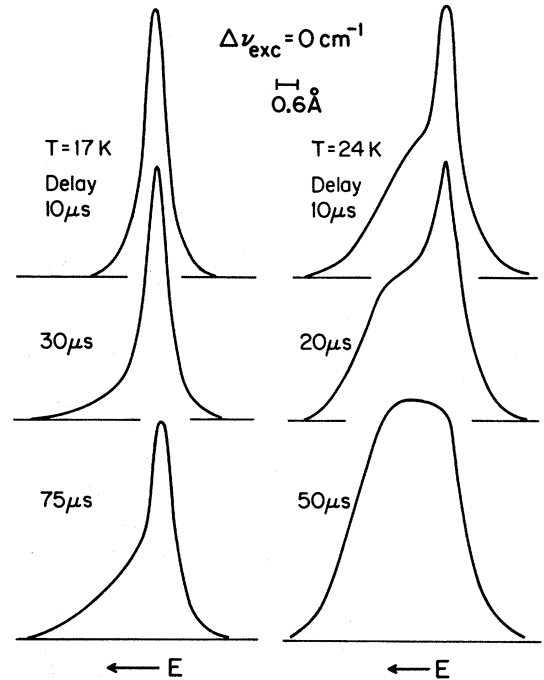
transfer becomes too fast for a meaningful determination of $R(t)$. This shows that the donor-donor transfer is strongly temperature dependent and justifies the assumption of fast donor-donor transfer at RT. For an accurate extraction of $R(t)$, excitation in the high- or low-energy wings of the inhomogeneous line is preferred. However, upon excitation in these wings, with $\Delta\nu_{exc}=+3$ and -2 cm^{-1}, very fast and slow, respectively, spectral diffusion was observed compared to transfer after line-center excitation at the same temperature (20 K). The spectral development for $\Delta\nu_{exc}=+3$ cm^{-1} also showed transfer (Fig. 8) across an inhomogeneous line within the main excitation spectrum profile and with a peak position different from that of the main line. Poor spectral isolation of the FLN component from the main line complicated determination of $R(t)$ and hence line-center excitation was used. This anomalous transfer indicates the existence of a separate domain in the main inhomogeneous envelope within which faster spectral transfer occurs, possibly because of a higher local Nd^{3+} concentration. This variation in transfer rates is consistent with the earlier mentioned variation of lifetimes across the inhomogeneous line at low temperatures, which was also described to a distribution in the Nd^{3+} concentration.

The time-resolved spectra in Fig. 7 show an asymmetrical and nonuniform rise in the background. In order to determine the donor-donor interaction mechanism, introduction of the quantity $R(t)$ in Eq. (4) is meaningful only under certain conditions.[24] Particularly relevant to this case it is assumed that the donor-donor transfer rates are independent of the energy mismatch between the two donors and that microscopic strain broadening determines the energy levels of the ions. If these two conditions are satisfied, the full inhomogeneous background rises uni-
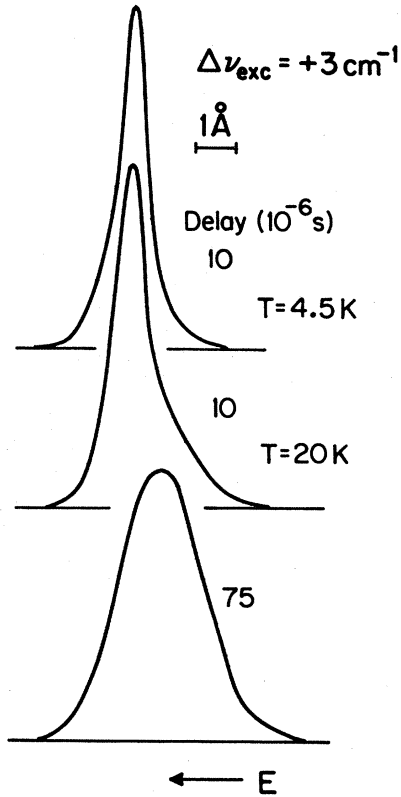
FIG. 8. TRFLN spectra at 20 K with excitation $+3$ cm^{-1} on the high-energy side ($\Delta\nu_{exc} = +3$ cm^{-1}) for $x=0.2$ sample. Upper trace shows FLN component in absence of spectral transfer at 4.5 K.
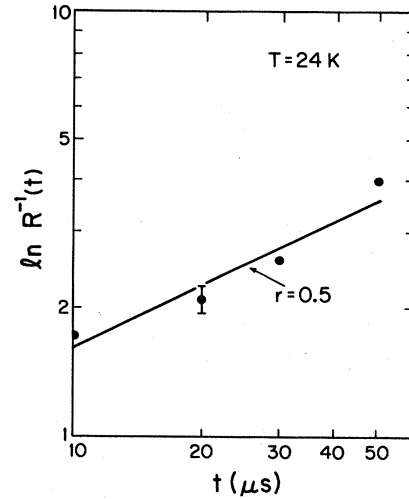

FIG. 9. Measured $R^{-1}(t)$ at 24 K for $x=0.2$. Slope of the straight line is given by $r=3/s$, indicating a dipole-dipole character for the donor-donor interaction.

TRFLN measurements. The product in Eq. (4) is again evaluated over a sufficiently large number of lattice sites to ensure convergence and a least-squares fit of the measured $R(t)$ values yields $W_{01}(T)$. This procedure is repeated for different temperatures and the NN donor-donor transfer rates are extracted for $17 < T < 24$ K. The results are shown in Fig. 10 and the data are fit to an ex-

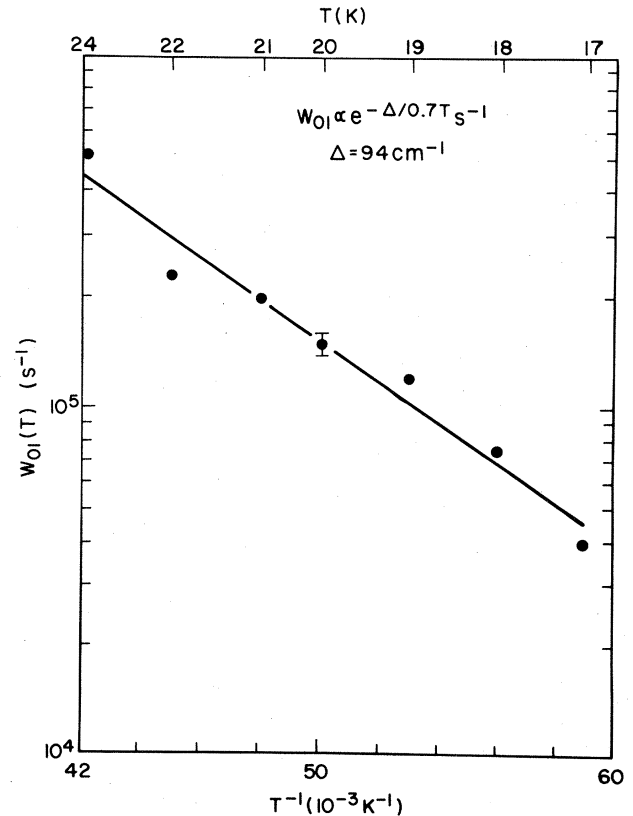formly, as is observed in all but a very few similar energy transfer studies.[28] The observed asymmetry and nonuniform rise in the TRFLN spectra appear to cast doubt on these conditions and could suggest energy-mismatch-dependent transfer mechanisms in LNPP. The spread in Nd^{3+} concentration and the possible presence of domains in the inhomogeneous line, however, complicate a description of the spectral dynamics with models which take this (possible) energy-mismatch-dependent transfer into account.[24] Similarly, the difference between the position of the FLN line and the peak of the inhomogeneous line in the long delay $^4F_{3/2}(1) \rightarrow {}^4I_{9/2}(1)$ spectra (Fig. 7) may be due to this variation in Nd^{3+} concentration and macroscopic broadening effects. These effects were ignored in the analysis of the ratio of the integrated FLN line intensity and the total integrated intensity. Hence the conclusions drawn from this analysis, regarding the specific interaction mechanism, should be considered as pertaining to an average over the inhomogeneous line.

$R(t)$ was determined from the TRFLN spectra and fit to the expression in Eq. (4). The multipolarity s of the donor-donor interaction was obtained[24] from a log-log plot of $R^{-1}(t)$. Figure 9 shows the $R^{-1}(t)$ data at 24 K. The slope r of this curve, which is given by $r=3/s$, indicates the electric dipole-dipole character ($s=6$) of the donor-donor transfer rate W_{0l}. X_{0l} is given by Eq. (3) with $X_{01} = 1.1 \times 10^3$ s^{-1} from the low-temperature

FIG. 10. NN donor-donor transfer rate $W_{01}(T)$ showing an exponential temperature dependence with an activation energy of $\Delta = 94$ cm^{-1}.

ponential behavior with an activation energy $\Delta = 94$ cm^{-1}:
$W_{01}(T) = 0.12 \times 10^9 \exp(-\Delta/0.7T)$.

Considering the small temperature interval over which the transfer rates were measured and the accuracy of the data, a reasonable fit of the $W_{01}(T)$ data could also be obtained with a T^7 dependence. The temperature dependence of $W_{01}(T)$ determines the specific phonon-assisted interaction mechanism. An overview of the various processes is given by Holstein et al.[29] The measured distance dependence of W_{0l} and the phase factors kr and $k'r$ of the phonons involved[30] indicate that the one-site resonant and the one-site nonresonant processes[29] are the possible transfer mechanisms. Both of these processes show an energy-mismatch-dependent transfer rate which could be consistent with the nonuniform use of the background. Energy transfer measurements in Nd^{3+}:YAG and Nd^{3+}:yttrium gallium garnet showed[31,32] that the one-site resonant mechanism is responsible for the spectral donor-donor transfer. In this two-phonon assisted process, a phonon resonant with the $^4I_{9/2}(2)$-$^4I_{9/2}(1)$ Stark splitting is absorbed, which corresponds to the activation energy Δ. This splitting was found to be 86 cm^{-1} in LNPP, which is within the error bar of the 94-cm^{-1} activation energy extracted from the $W_{01}(T)$ data. The donor-donor transfer mechanism in LNPP is therefore probably the one-site resonant process, although the one-site nonresonant process cannot be excluded.

Another argument favoring the resonant process follows from a comparison of the measured $W_{01}(T)$ with the FWM results.[15] These spatial migration studies yielded a RT value for the diffusion coefficient D for $x=1$. Huber showed[33] that in the presence of anisotropic diffusion an effective isotropic diffusion coefficient D_{eff} can be defined by

$$D_{\text{eff}} = \frac{D_2^{1/2}(D_3-D_1)^{1/2}}{F} . \quad (6a)$$

F is an incomplete elliptic integral of the first kind which is independent on D_i, $i=1,2,3$. In this expression D_1 is the smallest and D_3 is the largest of the three diffusion coefficients D_x, D_y, and D_z. In the case of an electric dipole-dipole interaction,[24] these are given by

$$D_i = \tfrac{1}{2}\beta \sum_l \frac{(R_{0l})_i^2}{(R_{0l_i})^6}, \quad i=x,y,z . \quad (6b)$$

Evaluating the lattice sums in Eq. (6b) and using the values of D from the FWM studies, the room-temperature value β(RT) can be extracted from which W_{01} ($T=300$ K) follows, using Eq. (5): W_{01} ($T=300$ K) $=1.45 \times 10^9$ s^{-1}. The TRFLN data show W_{01} ($T=20$ K) $=1.5 \times 10^5$ s^{-1}. The latter can be extrapolated to RT and compared with the FWM result. With the use of the exponential temperature dependence of the resonant process, a value for W_{01} ($T=300$ K) is obtained, which is ≈ 20 times smaller than the FWM value. Repeating this procedure with the T^7 dependence of the nonresonant process yields a W_{01} ($T=300$ K) which is $\approx 10^4$ times larger than the FWM value. It should be added that such an extrapolation can be qualitative at best, of course, since at higher temperatures, for example, effective donor concen-

tration decreases due to thermal population of the $^4I_{9/2}(2)$ and higher Stark levels.[34] In addition, the T^7 behavior applies only to the regime $T < 0.5T_D$ where T_D is the Debye temperature.

IV. CONCLUDING REMARKS

We have reported in this paper on the first, *direct* investigation of spectral dynamics in the $^4F_{3/2}(1)$ state of La$_{1-x}$P$_5$O$_{14}$:Nd$_x^{3+}$. The technique of TRFLN was applied resonantly in this inhomogeneously broadened state to study the anomalous exponential fluorescence decay and linear concentration quenching. At temperatures below 20 K no spectral diffusion was observed in $x=0.2$, 0.75, and 1.0 samples. This indicates an absence of fast, spectral, donor-donor energy transfer. In this temperature region the fluorescence decay of the FLN component was observed to be exponential and the concentration quenching rate is linearly dependent on the fractional concentration x. This unusual decay and quenching in the absence of fast donor-donor migration is explained by the generalized Inokuti-Hirayama model. In the limit of $\tau_0 \lesssim X_{01}^{-1}$ (the early-time regime) this model described an exponential decay and a linear quenching rate. The temperature-independent NN trapping (donor-acceptor) rate X_{01} is obtained from other, RT quenching rate measurements and is utilized in the calculation of the quantity $R(t)$ at low temperatures. The results of this calculation showed an exponential decay within the lifetime of the $^4F_{3/2}(1)$ state, which is consistent with the low-temperature TRFLN data. The calculation also shows a linear quenching rate for $0.01 < x < 1.0$ and does not indicate a break into a quadratic quenching rate at low concentrations, as claimed recently.[35]

At 20 K spectral diffusion was observed in the $x=0.75$ sample for the first time in this compound and the presence of phonon-assisted energy transfer within the inhomogeneous line was established. With the use of TRFLN, the donor-donor transfer mechanism was studied in $x=0.2$ by measuring the temperature dependence of the NN donor-donor transfer rate W_{01} between 17 and 24 K. This transfer rate was obtained from fitting the measured $R(t)$ with a recently developed incoherent energy transfer model for disordered systems. Excitation in the wings of the $^4F_{3/2}(1)$ excitation profile showed anomalously slow or fast transfer, compared to transfer following excitation at line center. This effect and a variation of the decay rate across the inhomogeneous line indicate the presence of domains of different Nd^{3+} concentration within the main line. The spectral development of the inhomogeneous background showed an asymmetrical and nonuniform rise with excitation at line center. Therefore, the presence of energy-mismatch-dependent spectral transfer cannot be excluded, but was not taken into account in the analysis of $R(t)$ because of the presence of these domains. The resulting $W_{01}(T)$ data were fit to a thermally activated behavior: $W_{01}(T) \sim \exp(-\Delta/0.7T)$ over the measured temperature range, although a reasonable fit could also be obtained with a T^7 dependence. These two dependencies correspond respectively to the one-site resonant and one-site nonresonant processes. A comparison with FWM

studies at RT and with energy transfer studies in other Nd^{3+}-doped systems favor the one-site resonant process as the donor-donor transfer mechanism in LNPP. However, the one-site nonresonant process cannot be excluded within the accuracy of the data. The spectral diffusion data correspond to a diffusion coefficient which decreases strongly with decreasing temperature. This conflicts with a recently observed diffusion coefficient *increasing* with *decreasing* temperature in the FWM experiments.[35] The latter diffusion coefficient corresponds to spatial migra-

tion, whereas our TRFLN result pertains to spectral migration. The relationship of spatial and spectral migration is influenced by the strain broadening in the host lattice and is not a very well understood problem (e.g., microscopic versus macroscopic strain broadening).

ACKNOWLEDGMENT

*Present address: AT&T Bell Laboratories, Murray Hill, NJ 07974.

[1]H. G. Danielmeyer and H. P. Weber, IEEE J. Quantum Electron. QE-8, 805 (1972).

[2]S. R. Chinn, H. Y. P. Hong, and J. W. Pierce, Laser Focus 12, 64 (1976).

[3]S. R. Chinn and W. K. Zwicker, J. Appl. Phys. 52, 66 (1981).

[4]A. Lempicki, Opt. Commun. 23, 376 (1977).

[5]W. Lenth, G. Huber, and D. Fay, Phys. Rev. B 23, 3877 (1981).

[6]H. G. Danielmeyer, M. Blätte, and P. Balmer, Appl. Phys. 1, 269 (1973).

[7]J. Hegarty, D. L. Huber, and W. M. Yen, Phys. Rev. B 23, 6271 (1981).

[8]S. Singh, D. C. Miller, J. R. Potopowicz, and L. K. Shick, J. Appl. Phys. 46, 1191 (1975).

[9]I. A. Bondar, B. I. Denker, A. I. Domanskii, T. G. Mamedov, L. P. Mezentseva, V. V. Osiko, and I. A. Shcherbakov, Kvantovaya Elektron. (Moscow) 4, 302 (1977) [Sov. J. Quantum Electron. 7, 167 (1977)].

[10]J. M. Flaherty and R. C. Powell, Phys. Rev. B 19, 32 (1979).

[11]R. Flach, D. S. Hamilton, P. M. Selzer, and W. M. Yen, Phys. Rev. B 15, 1248 (1977).

[12]For a review on energy transfer in crystalline and amorphous systems, see Laser Spectroscopy of Solids, edited by W. M. Yen and P. M. Selzer (Springer, Berlin, 1981).

[13]A. Szabo, Phys. Rev. Lett. 27, 323 (1971).

[14]J. Hegarty, D. L. Huber, and W. M. Yen, Phys. Rev. B 25, 5638 (1982).

[15]C. M. Lawson, R. C. Powell, and W. K. Zwicker, Phys. Rev. B 26, 4836 (1982).

[16]S. J. Nettel and A. Lempicki, Opt. Commun. 30, 387 (1979).

[17]M. M. Broer, D. L. Huber, W. M. Yen, and W. K. Zwicker, Phys. Rev. Lett. 49, 394 (1982).

[18]R. D. Plättner, W. W. Krühler, W. K. Zwicker, T. Kovats, and S. R. Chinn, J. Cryst. Growth 49, 274 (1980).

[19]M. Blätte, H. G. Danielmeyer, and R. Ulrich, Appl. Phys. 1, 275 (1973).

[20]M. M. Broer, Ph.D. thesis, University of Wisconsin, 1982.

[21]D. S. Hamilton, P. M. Selzer, and W. M. Yen, Phys. Rev. B 16, 1858 (1977).

[22]M. M. Broer, C. G. Levey, and W. M. Yen, Rev. Sci. Instrum. 54, 2656 (1983).

[23]A. J. Silversmith, Liren Lou, and W. M. Yen, Phys. Rev. B 26, 2656 (1982).

[24]D. L. Huber, in Laser Spectroscopy of Solids, edited by W. M. Yen and P. M. Selzer (Springer, Berlin, 1981), Chap. 3.

[25]R. Parrot, C. Barthon, B. Canny, B. Blanzat, and G. Collin, Phys. Rev. B 11, 1001 (1975).

[26]H. Y. P. Hong, Acta Crystallogr. Sect. B 30, 468 (1974).

[27]Equation (4) is an extension of Eq. (3.12) in Ref. 24 to the case of a self-quenching system. The $\cosh(W_{0l}t)$ term arises from the back transfer to site 0 from site l and incorporates a multiple exchange between the two sites.

[28]M. Harig, R. Charneau, and H. Dubost, Phys. Rev. Lett. 49, 715 (1982).

[29]T. Holstein, S. K. Lyo, and R. Orbach, in Laser Spectroscopy of Solids, edited by W. M. Yen and P. M. Selzer (Springer, Berlin, 1981), Chap. 2.

[30]Assuming a linear dispersion for the acoustic phonon involved in the transfer process, the wave vector k is given by $k = \Delta/(\hbar v_s)$, with Δ the phonon energy and v_s the average sound velocity.

[31]L. D. Merkle and R. C. Powell, Phys. Rev. B 20, 75 (1979).

[32]M. Zokai, R. C. Powell, G. F. Imbusch, and B. DiBartolo, J. Appl. Phys. 50, 5930 (1979).

[33]D. L. Huber, Phys. Rev. B 26, 3937 (1982).

[34]W. M. Yen, in Spectroscopy of Rare Earth Ions in Crystals, edited by R. M. Macfarlane and A. A. Kaplyanskii (North-Holland, Amsterdam, in press).

[35]J. K. Tyminski, R. C. Powell, and W. K. Zwicker, in Proceedings of the International Conference on Lasers '82, New Orleans, edited by R. C. Powell (STS Press, McLean, Virginia, 1982).